ESTB performance under the October 30th 2003 geomagnetic super storm

Article *in* Space communications · January 2005

CITATIONS
0

READS
64

4 authors, including:

Manuel Hernandez Pajares
Universitat Politècnica de Catalunya
228 PUBLICATIONS **3,022** CITATIONS
SEE PROFILE

Jose miguel Juan
Universitat Politècnica de Catalunya
154 PUBLICATIONS **2,496** CITATIONS
SEE PROFILE

Jaume Sanz
Universitat Politècnica de Catalunya
140 PUBLICATIONS **2,454** CITATIONS
SEE PROFILE

Space Communications 20 (2005/2006) 7–16
IOS Press

ESTB performance under the October 30th 2003 geomagnetic super storm

M. Hernández-Pajares [a], J.M. Juan [a], J. Sanz [a] and Santiago Soley [b]

[a] *Research Group of Astronomy and Geomatics (gAGE), Technical University of Catalonia, C/. Jordi Girona 1-2, Mod. C3, Campus Nord, UPC, Barcelona, Spain*

[b] *Pildo Labs, Eurocontrol Experimental Centre, Bretigny, France*

Abstract. A regular EGNOS Test Bed (ESTB) data collecting, 24 h per week, and analysis campaign has been developed by Eurocontrol along 2002 and 2003. During this period a geomagnetic storm was experienced on October 29th–31st 2003, degrading the ESTB performance in Europe.

In this work we present a study of the effects of this storm in several European sites on October 30th. The ESTB performance is monitored from a network of GPS receivers widely distributed over Europe, including the ESTB reference stations (RIMS), and the geographical degradation of the accuracy is analyzed. Also, the correlation between the geomagnetic activity index with the number of events with protection level failures is shown. In the most severe stormy periods, the errors in the ESTB ionospheric corrections and its integrity bounds are analyzed to explain the peaks in the navigation system error, which produces Misleading Information events.

This study is devoted to analyze the performance of the ESTB system, which is a simple prototype of the "true" final EGNOS system with several design limitations.

Keywords: SBAS, ESTB, EGNOS, ionosphere, storm

1. Introduction

The Satellite Based Augmentation System (SBAS) transmit to final users SBAS messages with differential corrections and integrity data to enhance the positioning signals sent out by GPS systems, making them suitable for safety critical applications such as civil aviation. But large disturbances in the ionosphere (geomagnetic storms, scintillation) can seriously affect the System Performance.

The SBAS messages are split in two categories of corrections and integrity data: clock-ephemeris and ionosphere. Being the ionosphere the component more difficult to model. Ionospheric Vertical Delays (Total Electron Content –TEC–) and their integrity bounds are computed by the master station from a network of reference stations, with typical distances of hundreds of kilometers. And provided to the users on $5^\circ \times 5^\circ$ or $10^\circ \times 10^\circ$ grids (depending on the latitude), with a maximum update interval of 300 seconds.

Space weather disturbances such as solar flares, coronal holes and coronal mass ejections are the main causes of geomagnetic storms on Earth; where ejections of charged particles (in solar wind) and electromagnetic energy propagate towards the Earth and couple the outer magnetosphere with the ionosphere and inner layers of the Earth's atmosphere. In such circumstances, smooth variations on TEC can be replaced by rapid fluctuations, and some regions can experience significantly higher or lower TEC values than normal.

On October 28th 2003, an intense solar eruption (an X-flare) was detected in an active region which had grown to one of the largest group of sunspots ever seen by the Solar Heliospheric Observatory (SOHO) satellite [1]. It appeared as a bright flash in SOHO ultraviolet images. This sudden enhancement of the solar radiation in the X-ray and extreme ultra-violet band produced a sudden increase of the ionospheric electron density on the daylight hemisphere. In Fig. 1 the simultaneous effect of the 28th October X-flare on the Slant Total Electron Content (STEC) for two stations, several thousands of kilometers far away, is shown. Indeed, the ionospheric refraction computed from GPS double frequency carrier phase measurements experience a sudden increase of about 2 m of L1–L2 delay (3 m in L1 delay) after 11 h, coinciding with the X-flare detection.

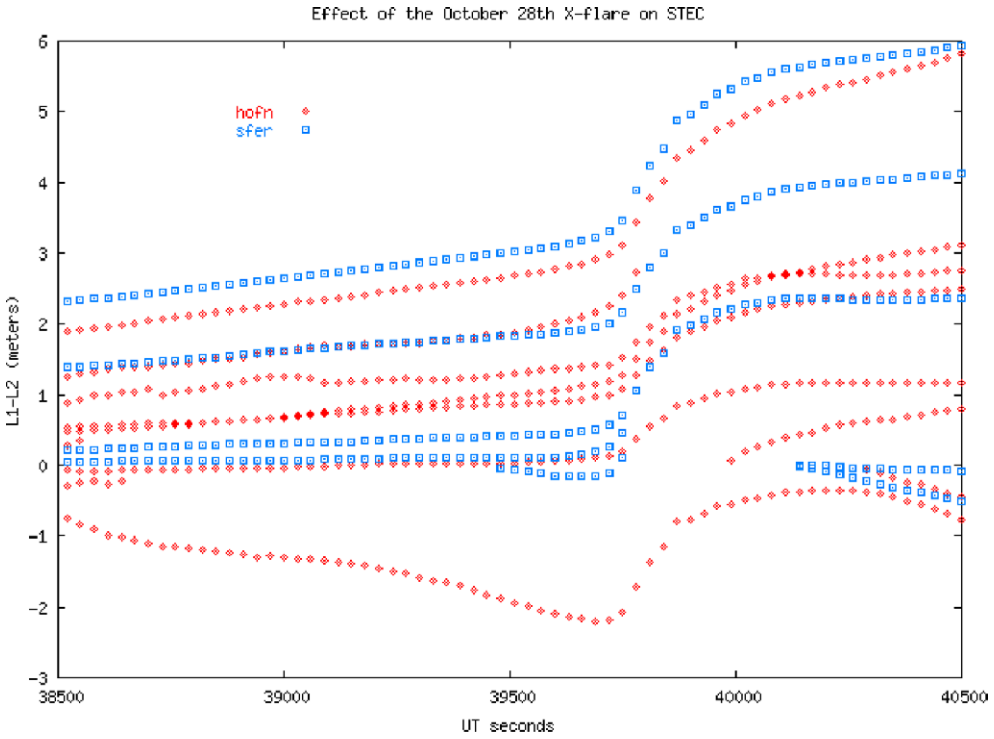

Fig. 1. Slant Total Electron Density (STEC) variations when the X-flare burst happened after 11 UT (39,600 seconds of day) of October 28th. The STEC has been computed from phase measurements (L1–L2) of satellites in view from two stations in Europe: hofn (Lon $= 345^\circ$, Lat $= 64^\circ$), diamonds, and sfer (Lon $= 354^\circ$, Lat $= 36^\circ$), squares.

Associated with the X-flare, a Coronal Mass Ejection occurred, which sent a large particle cloud impacting the Earth's magnetosphere about 19 hours later, on October 29th. Subsequent impacts were still occurring hours later. This material interacted with the Earth's magnetosphere, and a Storm Enhancement Density (SED) [2] coming from North America affected the northern latitudes in Europe at above 50 degrees in North latitude (see Fig. 2). And, extra large gradients of TEC associated with this phenomenon were produced, degrading the integrity and performance of GPS positioning.

During the storm, large values of the planetary Kp index (3-hourly index of geomagnetic activity) were experienced, reaching maximum levels of Kp $= 9$ during the most severe periods in October 29th and 30th.

The EGNOS Test Bed (ESTB) is a prototype of the final European Geostationary Navigation Overlay Service (EGNOS), developed as a main tool for supporting EGNOS design and demonstration users [3]. The impact of the October 30th storm over the ESTB performance is analyzed in this work in both, in the position and signal in space (SIS) domains.

2. The ESTB system

The ESTB became operational in February 2000, broadcasting MOPS [4,5] compliant SIS through INMARSAT Atlantic Ocean Region-East (AOR-E), until 2003 October 23rd, and afterwards was available through Indian Ocean Region-West (IOR-W).

As a prototype of the future final EGNOS system, the ESTB has several limitations. It works with a reduced number of reference stations (RIMS), about 12, regarding to the 34 RIMS for the final EGNOS one, and runs with a simple ionospheric algorithm. On the other hand, in the ESTB there are not elements to check the integrity of the information, while in EGNOS there are two elements devoted to integrity check: one with the EGNOS Central Processing Facility Processing Set (CPFPS) and the other on the complete EGNOS Central Processing Check Set (CPFCS).

This study has been carried out in the frame of the ESTB Data Collection and Analysis campaign of Eurocontrol, where several European centers are collecting and analyzing ESTB/EGNOS data since the 1st of January 2002. During two consecutive years 24 h, ESTB data sets were collected every week from Thurs-

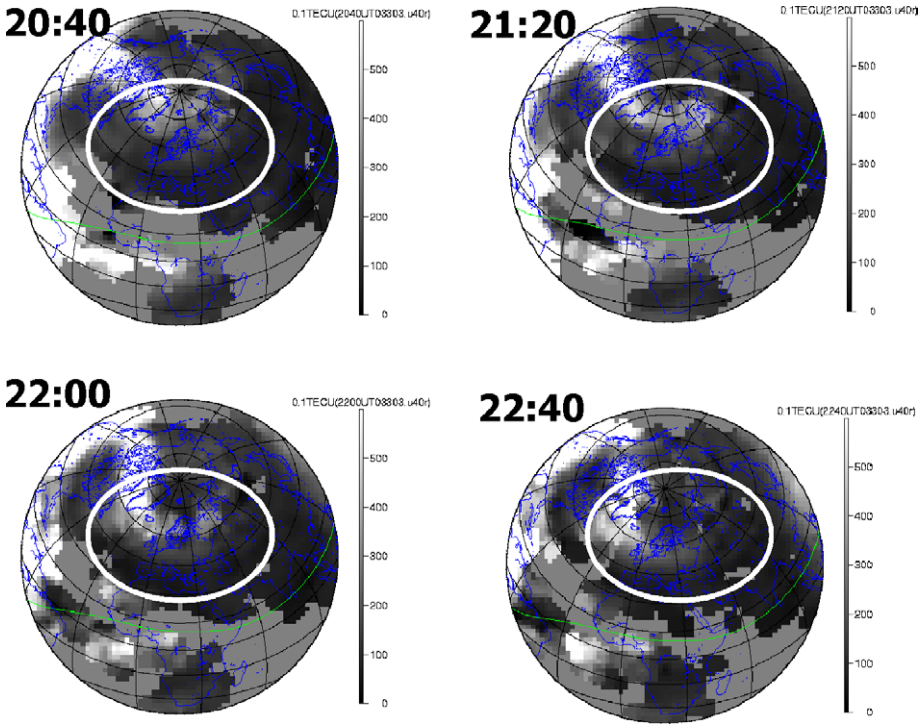

Fig. 2. Four snapshots of the Total Electron Content (TEC), every forty minutes, from 20:40 UT to 22:40 UT in October 30th 2003. The circle indicates the European region. Notice a SED coming from North America and reaching the northern European latitudes. The scale is given in tens of TECUs (1 TECU = 16 cm of L1 delay), from 0 to 600.

day 10 UT to Friday 10 UT and the ESTB performance was analyzed in both, in the position and the Signal in Space (SIS) domains. And, in particular, since the end of August of 2002, any potential anomaly detected in the collected data sets in Barcelona (Spain) was studied in detail to identify the potential causes: orbits and clocks, ionosphere, environment or processing software. This study revealed that, although the simple ionospheric algorithm implemented in the ESTB, the ionosphere was not an important source of problems for the ESTB integrity: only in two previous occasions, September 12th 2002 and August 21st 2003 the anomalies were related with the ionospheric corrections, but without producing a wide regional degradation as in the October 2003 storm [6]. A second super storm (not studied in this paper) was experienced on November 20th 2003, degrading also the ESTB performance over wide regions in Europe.

It must be pointed out that this study will be only devoted to analyze the ESTB performance, not the performance of the "true" final EGNOS system, i.e., the professional safety of life system, conceived with all safety consideration and design implications.

2.1. *The global monitoring system*

To provide a global monitoring of the ESTB or EGNOS Performance, gAGE/UPC, supported by PILDO Lab., has developed a Global Monitoring System (GMS) [7] under an Eurocontrol contract. This tool provides, on a daily basis, a wide SBAS performance monitoring over Europe using the different GPS/GEO data collection networks.

The measurement data files are gathered from public domain European ftp sites [8] or from the EGNOS Post Data Provider server [9], with the measurement files of the ESTB reference stations (RIMS). These files are combined with the collected GEO data from a SBAS receiver, or from a data server, and processed with BRUS [10] (a software package developed by gAGE/UPC for SBAS data processing). After computing the Navigation Solution, some statistic analysis and graphic results are generated and a data base is updated for further studies (see Fig. 3).

2.2. *Data processing*

During the October storm, the ESTB SIS were broadcasted by IOR-W in mode 2 (i.e., fast correc-

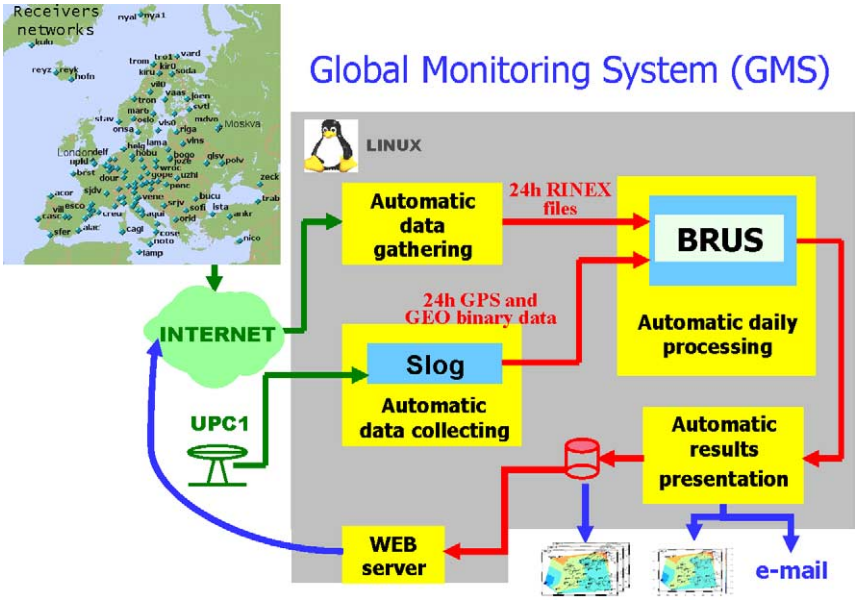

Fig. 3. Layout of the SBAS Global Monitoring System (GMS). The data sets from the GNSS receiver's networks are gathered from the Internet. These files are combined with the collected GEO data from a SBAS receiver and processed with the navigation software BRUS. After processing, some statistic analysis and graphic results are generated.

tions and ionosphere corrections with GEO Ranging), according to MOPS [5], with contents of a type 2 message in each type 0 message. Detailed information about ESTB signal schedule can be found in: http://esamultimedia.esa.int/docs/egnos/estb/schedule.htm.

The GMS was used to monitor the ESTB performance during the October storm, where data files from several European GPS receiver networks were combined with the GEO data and processed in such a way that a SBAS receiver was emulated at each site. Only the GEO ranging was out of the scope of such emulation, which did not affect the results because the GEO was not monitored at that time.

In order to improve the geographical coverage, sites at 30-seconds of sampling rate were included in the data sets beside the 1-second ones. Nevertheless, only the 1-second measurement files were taken into account when analyzing the integrity failures. The 30-seconds measurements were mainly used to help on the accuracy monitoring. Finally, most of the 1-second data files came from the ESTB Reference Stations used for generating the SBAS message; thence the best performance should be expected for such stations.

The data sets were processed in the Precision Approach mode, according to MOPS [5], but without applying smoothing to avoid any anomaly masking, and follow to the data processing strategy applied in the ESTB Data Collection and Evaluation Working Group [11] of Eurocontrol. Although the measurements were not smoothed, the receiver noise was set with the model defined in Appendix J.2.4 of [5] for the steady-state when the time constant is 100 seconds, and assuming the worst case signal reception conditions (i.e., $\sigma_{\text{noise,GPS}} = 0.4$ m and $\sigma_{\text{noise,GEO}} = 1.8$ m). As commented before, the software used for processing the GPS/GEO data was BRUS, but some data sets were also processed with an other independent software, PEGASUS [12] (using the same receiver noise model), to compare the results.

2.3. *The protection levels and integrity*

Integrity is the system's ability to provide warnings to the user when the system is unavailable for a specific operation. The SBAS system provides the users integrity information to compute the protection levels (Horizontal and Vertical Protection Levels, HPL and VPL), which represent an upper bound on its position error.

For each operation mode, Alarm Limits (AL) against which the user has to compare its Protection Levels are defined (ICAO's GNSS SARPS) [13], and the system is declared as Unavailable when the Protection Level is greater than the Alarm Limit. If the system is available and the Position Error is not bounded by the Protection Level, thence the event is considered as a HPL or VPL

failure, since the Protection Level is always supposed to be an upper bound of the Position Error. In such case, the event is declared as Hazardously Misleading Information (HMI) if the Position Error exceeds the Alarm Limit (which suppose an integrity risk), or as Misleading Information (MI) if the Alarm Limit is not exceeded (see Figs 5 and 6).

3. ESTB performance during the October storm

In Fig. 4 there is a map with the location of six European ESTB RIMS covering a wide range of latitudes from 40 to 70 degrees. The Stanford plots for such RIMS (24 h data of October 30th 2003) for the Horizontal and Vertical components are shown in Figs 5 and 6.

As it is shown in the Stanford plots, no HMIs were experienced in such RIMS for the Horizontal APV-II and Cat-I (HAL = 40 m) and for the Vertical APV-II (VAL = 20 m). That is, no integrity failures for such navigation modes were found. On the other hand, the error is below 5–10 meters in all the sites, except in "tro3". This station shows a worse performance due to its location in the border of the coverage area.

In Fig. 5 it can be seen that the Horizontal APVII and CAT-I availability is about 99% or greater in all the sites (99.9% in "tlse" and "palm") except in "tro3". On the other hand, MIs appear in the sites over 50 deg. In Fig. 6, it is shown that the vertical APV-II, is greater

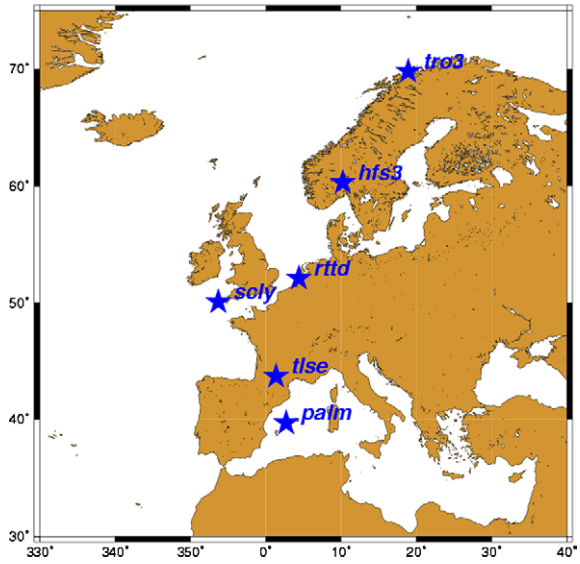

Fig. 4. Map with the location of the six European RIMS which Stanford plots are shown in Fig 5 and 6.

than the 99% in "palm" and in "tlse" (99,97%) and no MIs appears at such sites. Thence, the ESTB was able to achieve horizontal guidance APV-II and CAT-I in several RIMS and vertical APV-II in Toulouse ("tlse"), which was not strongly affected by the SED.

The impact of the storms over the integrity, measured in the number of protection level failures (XPE > XPL) in the Horizontal and Vertical components, and its relation with the Kp index is given in Fig. 7 for the European RIMS of Fig. 4. As it is shown, there is a great correlation in time between the periods with extreme values of Kp and the number of epochs with XPE > XPL. The events with VPE > VPL at the end of October 30th corresponds to the station "tro3", see Fig. 6.

The October's storm affected mainly to the European stations at high latitudes, especially at the end of October 30th 2003. In Fig. 8 two snapshots of the horizontal accuracy (95th percentile) can be seen for two time intervals of one hour. The first one, at left, corresponds to a quiet period in the afternoon, between 14 to 15 UT, in which the accuracy is keep into the nominal values, with degradation in the borders of the coverage area, in particular in the south-east (Mid East) and south-west (Canaries islands). The second one, at right, corresponds to a very active period, between 21 to 22 UT, in which the SED reached the north of Europe, seriously degrading the accuracy of ESTB at latitudes above 50 degrees. These large errors (between 5 to 10 meters) were found until 01 UT of October 31st 2003.

In Fig. 9, at top left, the HPE and HPL, computed from the ESTB data, are shown together with the standalone GPS solution for a permanent receiver in The Netherlands (Delft: lon = 4°5, lat = 52°). The figure corresponds to the time interval from 19 h to 22 h UT of October 30th, were several of the MIs in the Horizontal Stanford plots of Fig. 5 occurred ("rttd", "scly" and "tro3"). Notice that, although being more accurate the ESTB solution than the GPS standalone, both navigation solutions presents the same peak in the positioning error.

The ionospheric refraction computed from double frequency GPS code and phase measurements for several satellites in view (PRN15, 16, 18 and 02) used in the navigation solution is shown in the following plots of Fig. 9. The curves have been aligned with the STEC computed from the ESTB broadcasted data in order to compare the shapes of such determinations. The ESTB ionospheric bound, i.e., the User Ionospheric Range Error (UIRE), is also shown in the figure.

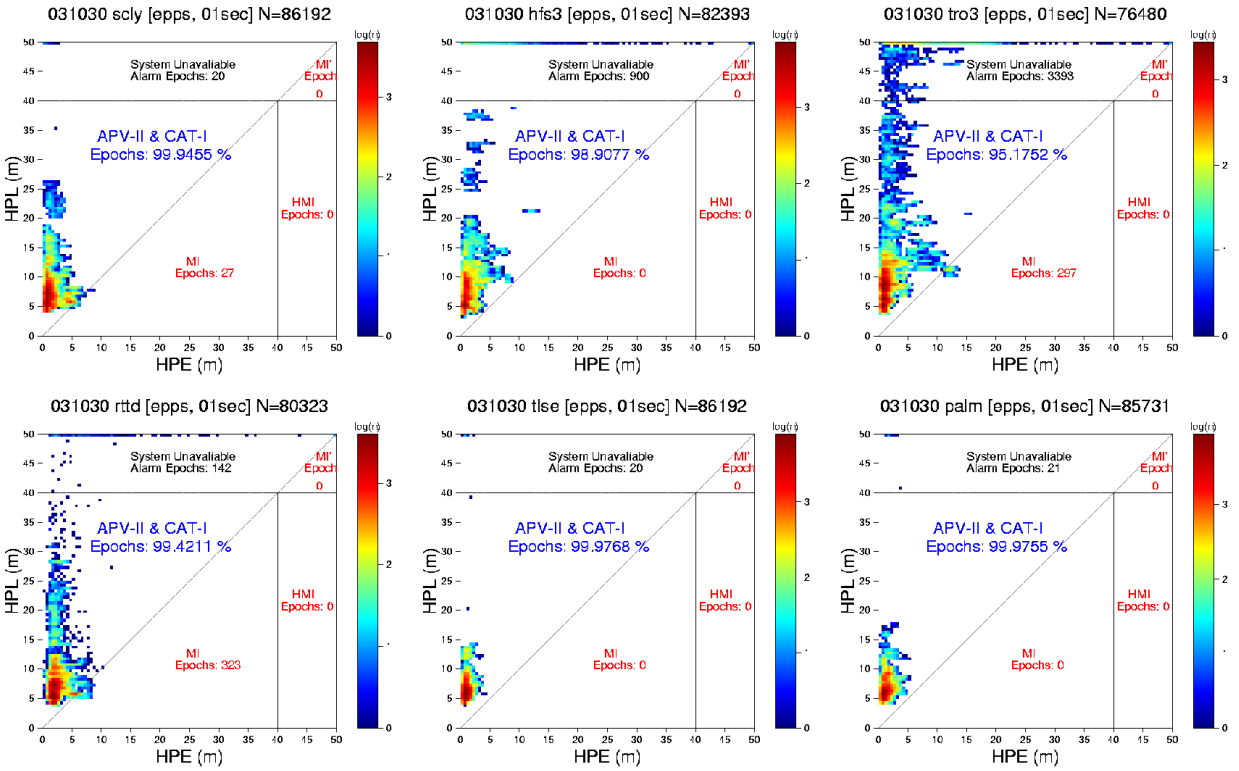

Fig. 5. Stanford Plot for the Horizontal component for the six ESTB RIMS of Fig. 4 (24 h data for 2003 October 30th). In the horizontal axis it is given the Horizontal Position Error (HPE) and in the vertical axis the Horizontal Protection Level (HPL), ranging from 0 to 50 m. The Alarm Limit is also shown in the plot as horizontal and vertical lines at 40 m. The MIs corresponds to the bins below the diagonal of the square and below the Alarm Limit. No HMIs occurs in these sites. The number of valid epochs N (i.e., in which the navigation solution has been computed) is indicated at top of each plot. The availability is also given as the percentage (%) over the valid epochs.

At top right of Fig. 9, a map is provided to show the discrepancies between the ESTB Vertical Delays (Total Electron Content –TEC–) and the TEC computed from the Global Ionospheric Maps (GIMs) provided by International GPS Service (IGS) [14]. The ionospheric Pierce Points (IPP) for the satellites in view are also included in the map. Under normal conditions, the accuracy of TEC computed from the IGS GIMs over Europe is about 3 TECUs (less than 0.5 meters of L1). Under storm conditions, the accuracy is worst, but they can still be used as a rough reference to provide a first glance of the ionospheric determinations error distribution. As it can be seen in Fig. 9, the peak in the HPE also appears in the ionospheric refraction plots of satellites PRN15 and PRN18 computed by GPS double frequency code (P2–P1) and phase measurements (L1–L2).

Such peaks last for about ten or fifteen minutes in time and involve an increment of the ionospheric delay of about 10 m in L1. This fast variation of the ionospheric refraction is not followed by the ESTB STEC (and also the UIREs are not inflated properly), degrading the accuracy of the navigation solution. Nevertheless, as it can be appreciated in the figure, there is an increase of the UIRE by the time of the peaks in XPE, which means that the system is reacting somehow to increase the error, but, finally it is not enough to bound it.

On the other hand, not all the satellites in view are affected in the same way by the ionospheric TEC gradients. For instance, no peaks appear when analyzing the ionospheric refraction plots of satellites PRN02 and 16, which show very flat patters for three hours.

The ionospheric refraction for several consecutive days (from October 27th to November 1st 2003) is shown in Fig. 10 for the satellites PRN02, left, and PRN15, right, in order to compare the different behaviour of the STEC around the storm. The plots show shifted curves of L1–L2 (from double frequency GPS carrier phase measurements).

As it can be seen, the curves have singular patterns during the stormy days (October 29th, 30th 31st).

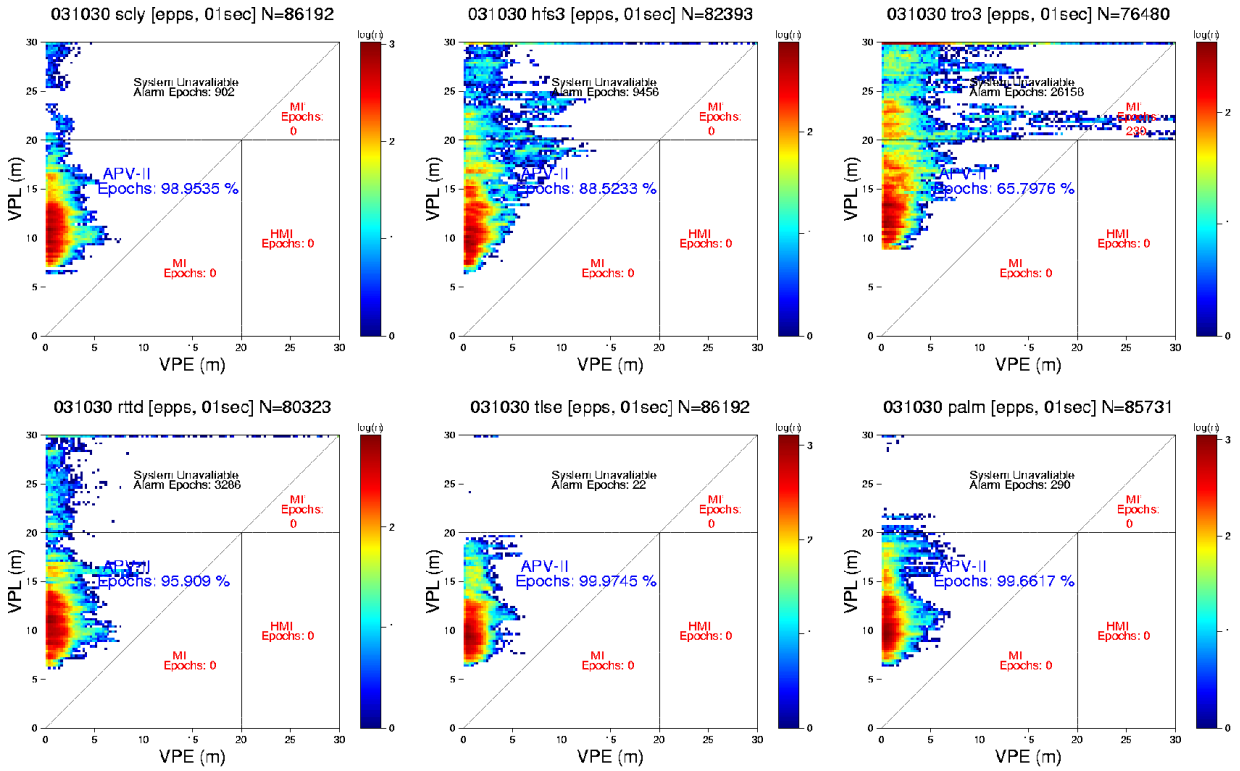

Fig. 6. Similar plots than in Fig. 4, but for the vertical APV-II. The VPE and VPL range from 0 to 30 m, and the AL is set at 20 m.

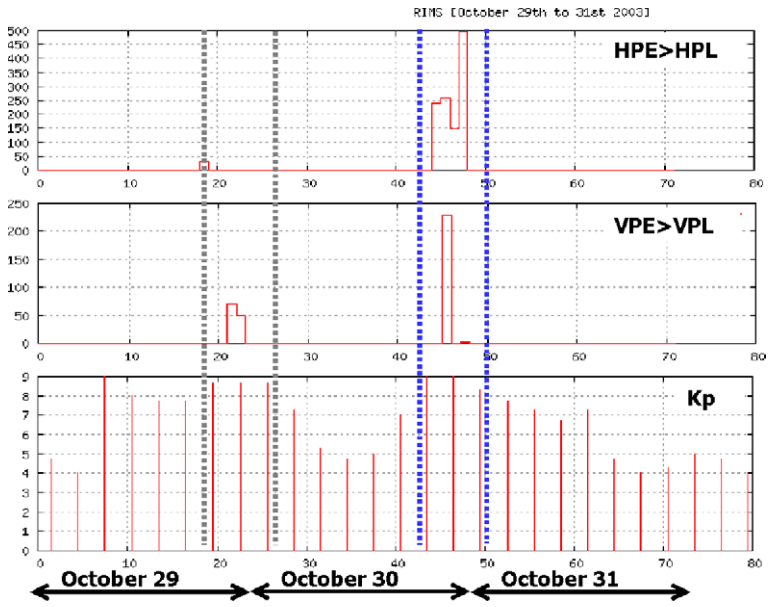

Fig. 7. Relation between the number of events with XPE $>$ XPL in the Horizontal (at top) and Vertical (middle) error components, and the Kp index during the last three days in the end of October 2003. All RMS of Fig. 4 have been included in this plot. The vertical scales ranges values between 0 to 500 events for the Horizontal component, between 0 to 250 events for the Vertical component, and 0 to 9 for the Kp Index. No HMIs were experienced in such RIMS in the Horizontal APV-II and Cat-I (HAL $=$ 40 m) and Vertical APV-II (VAL $=$ 20 m).

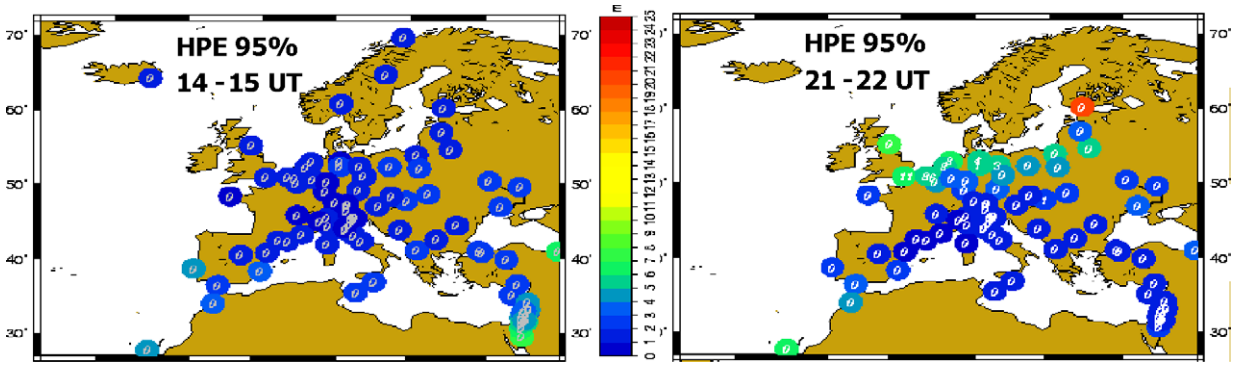

Fig. 8. Two snapshots of the ESTB Performance (horizontal accuracy: 95th percentile) in October 30th 2003. The color scale for HPE is given in meters, ranging from 0 to 25 m. All available stations, with measurements at 1 sec and 30 sec, have been used in this plot.

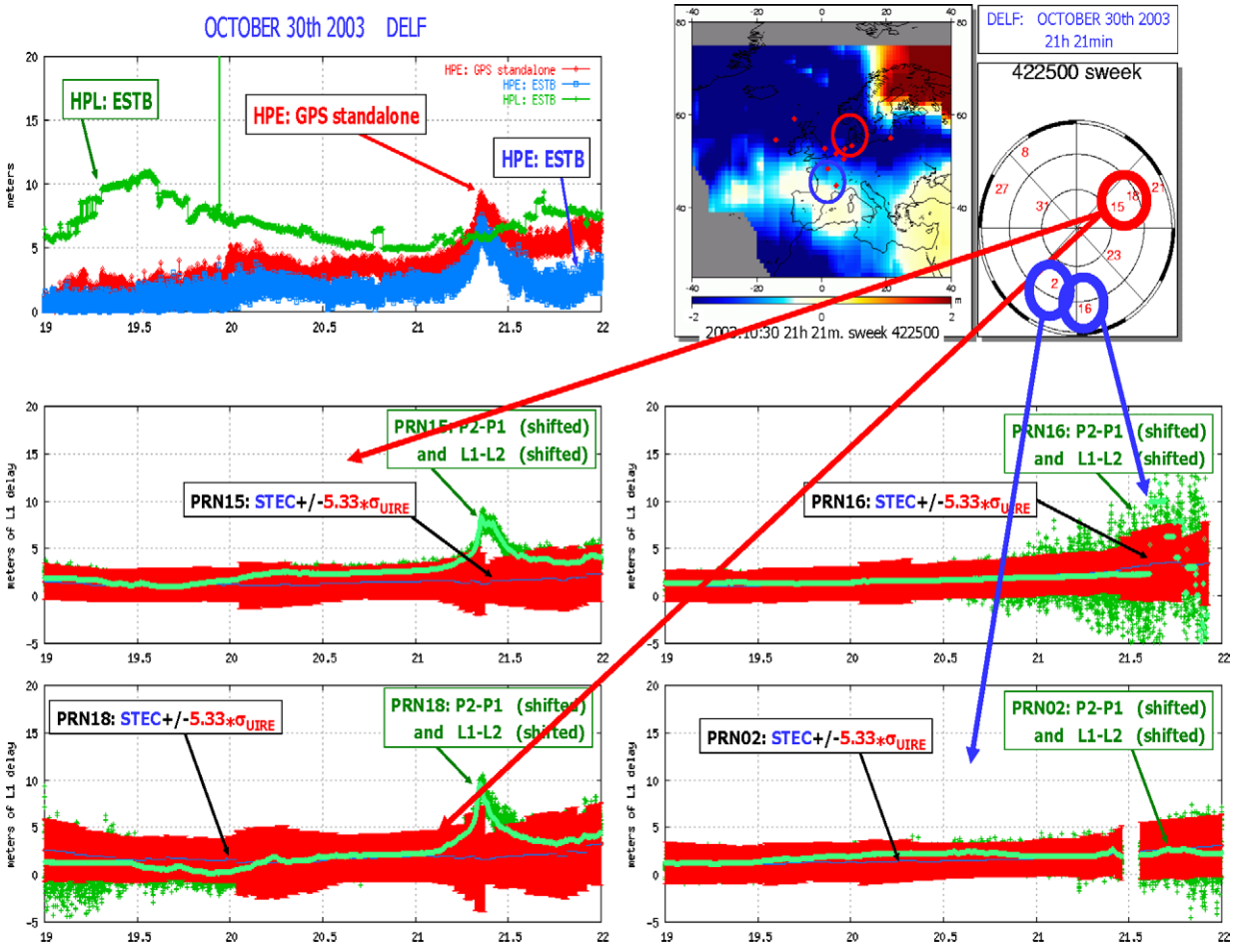

Fig. 9. Delft (Netherlands), October 30th 2003. At top left: GPS standalone HPE and the ESTB HPE/HPL, from 19 to 22 UT. Next two rows: The ESTB STEC with the confidence bound (UIRE) is compared with the ionospheric refraction computed from code (P2–P1) and phase (L1–L2) measurements for satellites PRN15, 18, 16 and 02. At top right: map with the discrepancies between the ESTB and IGS vertical delays (in meters of L1 delay, color palette saturating at ± 2 m of L1). The IPPs are also given in the map. Beside the map, a sky plot is provided with the satellites used in the navigation solution to show the geometry of the satellites in view from Delft, and to identify the IPPs in the previous map (notice that the projection is quite different).

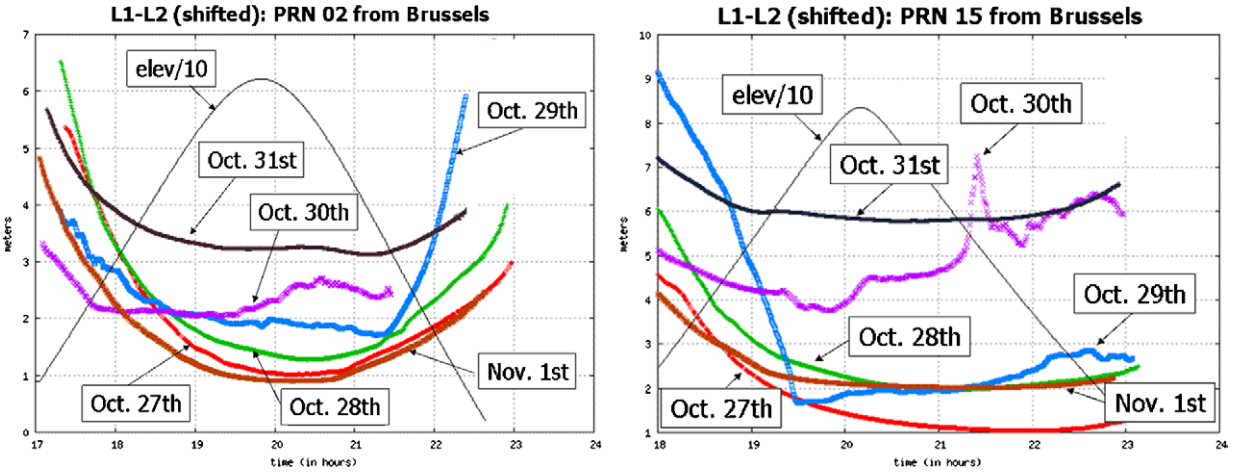

Fig. 10. Ionospheric refraction computed from double frequency carrier phase GPS measurements L1–L2 (shifted), for two satellites in view from Brussels: PRN02 (left) and PRN15 (right). Each curve corresponds to a different day from October 27th to November 1st 2003. The horizontal axis is given in hours into the day (from 17 to 24 UT), and the vertical axis in meters of L1–L2 delay (1 meter of L1–L2 delay is about 1.5 m of L1 delay). The satellite elevation (divided by ten) is also shown in the map.

There are very flat and, basically, without changing with the elevation for a long period (about two hours). This feature reveals a very low electron density in the sounded region of the ionosphere. And, on the other hand, sudden changes appears in few minutes (such elbows), which means strong gradients in the ionosphere.

From the scatter plot and the map at top of Fig. 9, it can be seen that the satellites PRN15 and 18 have IPPs close together, which are located in a region with large discrepancies between the ESTB and the IGS TEC determinations. Instead, the other satellites, PRN02 and 16, are located in another region with lower discrepancies. It must be pointed out that the discrepancies map does not provide the actual error of the ESTB TEC. It only provides the discrepancies between the ESTB and IGS TEC determinations, and both could be biased for instance, at the same time. Anyway the regions in which large discrepancies appear can be viewed as an indicator of the areas more difficult to model due to fast variations or big gradients of TEC. And the regions with low discrepancies, as those where the determinations are, probably, more accurate. This is compatible with the absence of the peak in the STEC of satellites PRN02 and 16, which pierce a region with low discrepancies.

4. Conclusions

A geomagnetic storm was experienced on October 29–31st 2003, with large oscillations on 30th, and presenting a Storm Enhancement of Density (SED), coming from North America and affecting the northern latitudes in Europe above 50 degrees.

The ESTB performance has been monitored on October 30th 2003 from a network of GPS receivers wide distributed over Europe, including the ESTB reference stations, between 40 to 70 degrees in latitude, in such a way that a SBAS receiver was emulated at each site.

In the position domain, Horizontal APV-II and CAT-I was achieved in several RIMS. And Vertical APV-II guidance was also achieved in the RIMS "tlse" (99.97%) and "palm" (99.66%), who were basically not affected by the SED. On the other hand, and although no integrity failures (HMIs) were experienced in the analyzed European RIMS, several MIs occurred in the RIMS over 50 degrees of latitude, which were highly correlated in time with the periods with extreme values of Kp in both storms.

In order to explain the MIs observed in the RIMS affected by the SED at the end of October 30th, the ESTB Slant Total Electron Content has been compared with the ionospheric refraction computed from double frequency GPS code and phase measurements for a permanent receiver in Delft (The Netherlands). Only the shape of such determinations has been compared, which is enough to illustrate the magnitude of the errors, which are not bounded by the confidence values, producing the MIs. Also a map with the discrepancy between the ESTB and IGS vertical delays (TEC) has been also generated to help the analysis of the geographical distribution of the satellites that contributes to the MIs.

From this study we can conclude that, although being the ESTB a simple prototype of the final European SBAS system EGNOS, and taking into account the strength of the analyzed storm, it was performing well in such difficult scenario.

Acknowledgment

This work has been partially supported by the EUROCONTROL Contract Numbers C/1.239/CE/JR/01 and C/1.057/CE/JR/03, and by the Spanish projects PETRI (95-0722-0P-01) and the ESP2004-045682-C02-01.

We thank the IGS community for providing the ground receiver data.

References

[1] SOHO: http:// sohowww.nascom.nasa.gov.

[2] J.C. Foster, P.J. Erickson, A.J. Coster, J. Goldstein and F.J. Rich, Ionospheric signatures of plasmaspheric tails, *Geophysical Research Letters* **29**(13) 1623, 10. 1029/ 2002GL015067, 2002.

[3] http://esamultimedia.esa.int/docs/egnos/estb/esaEG/estb.html.

[4] Minimum Operational Performance Standards for GPS/WAAS Airborne Equipment, RTCA, Do 229A, June 1998.

[5] Minimum Operational Performance Standards for GPS/WAAS Airborne Equipment, RTCA, Do 229B, October 1999.

[6] EUROCONTROL: http://www.eurocontrol.fr/projects/sbas.

[7] *Software User Manual GMS*, Doc.-No.: GMS_SUM-01. sigue A.

[8] Public GPS data servers: lox.ucsd.edu (lox), cddisa.gsfc. nasa.gov (cddisa), lareg.ensg.ign.fr (lareg), geodaf.mt.asi.it (geodaf).

[9] The ESTB Post Data Provider Server (account and password is needed): http://estbsrv.gdiv.statkart.no.

[10] Basic Research Utilities for SBAS (BRUS), M. Hernández-Pajares, J.M. Juan, J. Sanz, X. Prats and J. Baeta, in: *Geomatics Week*, Barcelona, Spain, 2003.

[11] Data Collection Report Proposed Template, EEC GOV Working Group Is.1 Rev. 1.

[12] Interface Control Document, EEC PEGASUS, Doc.-No.: PEG-ICD-01 issue E.

[13] Draft SARPS for Satellite Navigation Systems, in: *ICAO GNSS Panel*, Montreal, 1999.

[14] M. Hernandez-Pajares, IGS Ionosphere WG position paper: present and future activities, in: *Proceedings of the IGS Technical Meeting*, Bern, Switzerland, 2004.